

Atomic structure of Tb(11 $\bar{2}$ 0)

Y. S. Li, J. Quinn, and F. Jona

College of Engineering and Applied Science, State University of New York, Stony Brook, New York 11794

P. M. Marcus

IBM Research Center, Yorktown Heights, New York 10598

(Received 27 February 1992)

A low-energy electron-diffraction intensity analysis of a Tb(11 $\bar{2}$ 0) surface finds that the atomic structure of this surface is different from bulk structure in two ways: The spacing between the first and the second layer, which have two inequivalent atoms in the unit mesh, is contracted by 3.3% (0.06 Å), and the two inequivalent atoms in the first layer translate parallel to the surface by equal and opposite amounts of 0.21 Å. Thus the change in registration of the composite surface layer preserves both the size and the symmetry of the unit mesh of parallel bulk layers. This kind of surface rearrangement is different from that reported by others for the (11 $\bar{2}$ 0) surfaces of other rare-earth metals, such as Y, Gd, and Ho.

I. INTRODUCTION

Studies of the atomic and electronic structure of surface of the rare-earth metals have lagged behind those of other metals¹ for experimental reasons: the growth of large (several-mm) single crystals with high and ultrahigh purity is difficult and expensive,^{2,3} and the preparation of atomically clean surfaces is difficult, extremely time consuming, and still not well established. Progress has been slow and some of the published results are often controversial and unconfirmed.

Qualitative low-energy electron-diffraction (LEED) observations and angle-resolved photoemission measurements on surfaces of Y, Pr, Gd, Ho, and Er have been reported by Blyth *et al.*⁴ and Barrett *et al.*⁴ Quantitative results, however, are available only for two rare-earth surfaces, namely, the (0001) surfaces of hexagonal close-packed (hcp) Sc (Ref. 5) and Tb (Ref. 6), both results obtained by means of LEED intensity analyses. These results fit well in the norm of what is known about basal-plane surfaces of hcp metals: both Sc(0001) and Tb(0001) are bulklike but relaxed, with the first interlayer spacing contracted 2% and 3.9%, respectively, with respect to the bulk.

The (11 $\bar{2}$ 0) surfaces, by contrast, seem to be anomalous. The qualitative LEED investigations⁴ have shown that Y(11 $\bar{2}$ 0), Ho(11 $\bar{2}$ 0), and Er(11 $\bar{2}$ 0) are reconstructed. The reconstruction involves a change of symmetry—the twofold-symmetric ideal (11 $\bar{2}$ 0) surfaces reconstruct to close-packed structures with sixfold symmetry, and the corresponding LEED patterns are very similar to those obtained from the corresponding (0001) surfaces. No quantitative structure determinations were done, but a visual comparison between the Ho(11 $\bar{2}$ 0) and the Ho(0001) LEED patterns at the same electron energy was reported to show that the lattice parameter of the reconstructed (11 $\bar{2}$ 0) surface was within a few percent of that of the (0001) surface.⁴

We report here the results of a quantitative study of Tb(11 $\bar{2}$ 0). The purpose of this study was threefold: (1) we wanted to see whether we could prepare an atomically clean Tb(11 $\bar{2}$ 0) surface suitable for structure studies; (2) if we could, we wanted to see whether this surface exhibits the same type of reconstruction that was reported for Y, Ho, and Er; and (3) we wanted to carry out a quantitative determination of the atomic structure of the clean surface. The experimental techniques used for this purpose were LEED and Auger-electron spectroscopy (AES).

In Sec. II we describe the bulk structure of Tb(11 $\bar{2}$ 0) and the notation used in this paper. In Sec. III we present the procedure followed for the preparation of an atomically clean surface and we give a few experimental details. In Sec. IV we report on the intensity calculations, the structure analysis, and its results. In Sec. V we summarize and discuss the results.

II. BULK STRUCTURE OF Tb(11 $\bar{2}$ 0)

The lattice parameters of hcp Tb are $a = 3.60$ Å and $c = 5.69$ Å, hence with axial ratio $c/a = 1.581$. A cut through a hard-sphere model of bulk Tb along a (11 $\bar{2}$ 0) plane is depicted in Fig. 1 [(a) top view and (b) side view].

We choose a Cartesian coordinate system with x and y in the (11 $\bar{2}$ 0) plane, the x axis along $\langle 1\bar{1}00 \rangle$, the y axis along $\langle 0001 \rangle$, and a z axis along $[11\bar{2}0]$, as indicated in the figure. The surface unit mesh is a rectangle with sides $a_1 = 2a \sin 60^\circ = 6.235$ Å and $a_2 = c = 5.69$ Å, and contains two atoms [labeled 1 and 1' in Fig. 1(a)] with coordinates (0,0) and $(a_1/3, a_2/2)$, respectively. The symmetry elements are a mirror plane (line) perpendicular to $\langle 0001 \rangle$ [dashed line coinciding with the x axis in Fig. 1(a)] and a glide plane (line) parallel to $\langle 0001 \rangle$ at location $x = a_1/6$ [vertical dashed line in Fig. 1(a)]. The translation vector from the origin in the first to the origin in the

second layer is $\mathbf{s}=(a_1/2, 0, -d_{\text{bulk}})$ with $d_{\text{bulk}}=a/2=1.80 \text{ \AA}$.

The geometry of the LEED pattern from Tb(11 $\bar{2}$ 0) is shown schematically in Fig. 1(c). The mirror line along \mathbf{k}_x makes the corresponding reflections above and below that line degenerate with one another. In addition, sys-

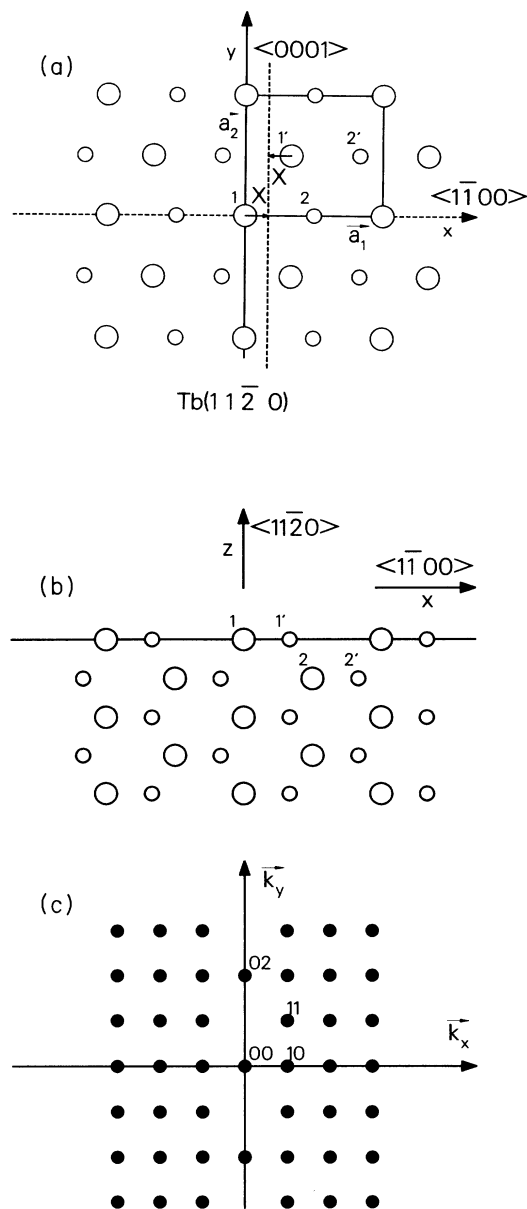


FIG. 1. (a) Schematic top view of Tb(11 $\bar{2}$ 0). Larger circles represent atoms in the first layer, smaller circles represent atoms in the second layer. The unit mesh, sides a_1 and a_2 , is indicated with solid lines. The x axis coincides with a mirror line. The vertical dashed line is a glide line. (b) Schematic side view of Tb(11 $\bar{2}$ 0). Larger circles represent atoms in the plane of the drawing, smaller circles represent atoms in the plane below. (c) Schematic LEED pattern from Tb(11 $\bar{2}$ 0).

tematic reflection absences are expected as a consequence of the glide line: with the choice of axes made in Fig. 1, absences are expected (and observed) in the beams with indices $0k$ with k odd. Additional extinctions would be expected to occur in the kinematic limit for an ideally bulklike surface, owing to the special relative positions of atoms 1 and 1', at the reflections hk such that $h/3 + k/2 = n + \frac{1}{2}$, i.e., with $h = 3n$ and k odd. These extinctions are not observed, however, for two reasons. The first reason is multiple scattering: even for an ideally bulklike surface a dynamical calculation shows that, e.g., the reflection 31 is weak, but not zero. The second reason is that on the (11 $\bar{2}$ 0) surface the relative positions of atoms 1 and 1' can vary, expectedly in such a way that both the mirror line and the glide line are maintained. For example, calling X the shortest distance from atom 1 and from atom 1' to the glide line [see Fig. 1(a), $X = a_1/6 = 1.04 \text{ \AA}$ in the ideally bulklike structure], a change ΔX of X would violate the extinction condition and produce a nonzero intensity in, e.g., the 31 reflection. We will see below that, in fact, ΔX is finite on the Tb(11 $\bar{2}$ 0) surface.

III. EXPERIMENT

A single-crystal ingot of Tb metal, purified by the method of solid-state electrotransport as described elsewhere,³ was oriented along a $\langle 11\bar{2}0 \rangle$ direction by means of Laue diffraction patterns. A platelet was then cut with a slow diamond wheel to dimensions $5 \text{ mm} \times 3 \text{ mm} \times 2 \text{ mm}$ and with the major surfaces perpendicular to a $\langle 11\bar{2}0 \rangle$ direction. One of these surfaces was lapped and polished in kerosene with diamond-powder slurries with successively decreasing grain sizes (3, 1, and $0.25 \mu\text{m}$) until the orientation was within 0.5° of a (11 $\bar{2}$ 0) plane. The finished surface was mirrorlike and blue-colored as discussed elsewhere.⁶ The platelet was then mounted in a sample holder by means of a 0.25-mm-diam Mo wire wrapped around the edges. The holder allowed heating of the platelet by electron bombardment of the back surface.

After attainment of base pressure ($< 1 \times 10^{-10}$ Torr), the polished surface was subjected to repeated bombardment with Ar ions (5×10^{-5} Torr, 375 V, $2 \mu\text{A}$) as described below, and was tested for impurities by AES using the LEED optics as a retarding-field analyzer (RFA). Figure 2 depicts AES scans taken at different stages of the cleaning process: Fig. 2(a) pertains to the starting condition of the surface (large Cl and O signals are visible). The concentrations of the main impurities, carbon, oxygen, chlorine, and iron, were monitored by the ratio between the intensity of the impurity's AES line and the intensity of the Tb AES line at 146 eV.

After four cycles of 20-h Ar-ion bombardments at 600°C followed by 1-h anneal at 600°C , chlorine was eliminated, but C, O, and Fe were still detectable with the following ratios: $R_C = I_{C(272 \text{ eV})} / I_{\text{Tb}(146 \text{ eV})} = 0.09$, $R_O = I_{O(510 \text{ eV})} / I_{\text{Tb}(146 \text{ eV})} = 0.07$, and $R_{\text{Fe}} = I_{\text{Fe}(47 \text{ eV})} / I_{\text{Tb}(146 \text{ eV})} = 0.04$. At this stage, no LEED pattern was observable from the sample surface. Indeed, the Fe signal could be eliminated from the AES spectra by 1-h Ar-

ion bombardment at room temperature, but of course no LEED pattern was observable. Figure 2(b) shows an AES scan taken after the four cycles mentioned above plus 1-h Ar-ion bombardment at room temperature.

To obtain a LEED pattern at all, it was necessary to anneal the sample at about 1000°C for 1 h. However, the pattern had only weak 1×1 spots and very high background sometimes with extra spots and with streaks perpendicular to the c direction of the hcp lattice. No improvement of the pattern was obtained with further anneals at temperatures between 550°C and 1000°C for time periods ranging from minute to hours. These observations were related to segregation of Fe during the annealing process, which increased the concentration of Fe on the surface, producing R_{Fe} values ranging between 0.1 and 0.3. Figure 2(c) shows an AES scan taken after 1-h

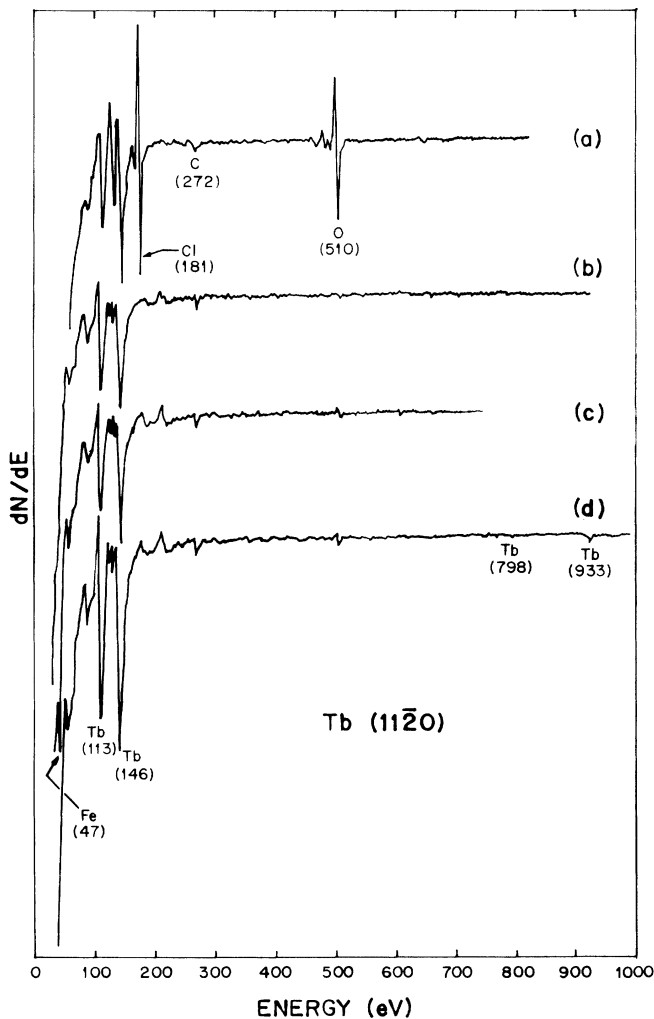


FIG. 2. AES scans of $Tb(11\bar{2}0)$ at different stages of the cleaning process. (a) Initial condition; (b) after four cycles of 20 h of Ar-ion bombardment at 600°C followed by 1-h Ar-ion bombardment at room temperature; (c) after 1-h anneal at 700°C (note the Fe line at 47 eV); (d) after the procedure described in the text.

anneal at 700°C. Note the presence of an Fe signal at 47 eV (the RFA is most sensitive to low electron energies and becomes increasingly insensitive at high energies, which explains why the Fe signals expected at 598, 651, and 703 eV are not detected).

A successful recipe for producing a clean and well-crystallized $(11\bar{2}0)$ surface was found to be the following. After the preliminary treatments described in the two preceding paragraphs, the routine procedure prior to data collection was to ion-bombard the surface for about $\frac{1}{2}$ h, anneal the surface at 1100°C for 10 min, and then cool the sample rapidly (from 1100°C to 550°C in 2 min or less). This treatment produced an Fe-free surface and a weak 1×1 LEED pattern with high background: on the fluorescent screen of our display-type LEED apparatus the diffraction spots were discernible, above background, only below 140 eV. A subsequent 3-h anneal at 400°C produced a 1×1 LEED pattern with strong beam intensities and low background, the pattern being visible up to electron energies of 300 eV. Figure 3 presents a photograph of the LEED pattern at 56 eV: note the extinction, discussed in the preceding section, of the 01 spot. After this treatment, the AES ratios were $R_C=0.09$, $R_O=0.07$, and $R_{Fe}=0$, which we define here as the state of an acceptably clean $(11\bar{2}0)$ surface. Figure 2(d) depicts the corresponding AES scan: note the absence of the Fe signal at 47 eV and the presence of the two small Tb peaks at 125–130 eV, which are resolved only when the impurity concentrations in the surface region are small.

The LEED intensity spectra [so-called $I(V)$ spectra] used in the analysis described below were collected from such a surface by means of a microcomputer-television-camera system as described elsewhere.⁸ Data collected with the sample at room temperature or with the sample at about -100°C were essentially identical to one another. Data were collected for a total of 23 LEED spectra for normal incidence of the primary electron beam and energies between 25 and 200 eV. Degenerate spectra were averaged to reduce the set to 11 nondegenerate $I(V)$ curves to be used in the analysis, namely, 10, 11, 20, 02, 21, 12, 22, 30, 13, 23, and 32. [The 31 beam, which should be particularly sensitive to the distance X of atoms 1 and 1' from the glide line (see Sec. II), was not used in the analysis because its intensity was very low and there-

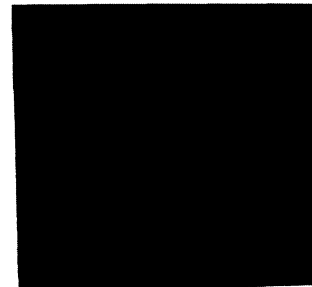


FIG. 3. Photograph of LEED pattern from clean $Tb(11\bar{2}0)$ for 56-eV incident electrons.

fore not measurable with sufficient accuracy.] These curves were then normalized to constant incident current, smoothed (by convolution of the experimental curves with Gaussian filter functions), and corrected to reduce the background to a minimum (the data-collection software subtracts on line the intensity in the vicinity of a LEED beam from the integrated intensity of that beam). The symmetry relations among the beams told us that the two symmetry elements of the bulk planes (mirror and glide) were present in the surface.

IV. STRUCTURE ANALYSIS AND RESULTS

The calculations of LEED intensities were done by means of the CHANGE computer program⁹ with eight phase shifts. The CHANGE program treats the scattering from each composite layer, made up of two elementary or Bravais nets in the same plane, in spherical waves, and the scattering between composite layers in plane waves (beams). The energy range was divided into three parts: from 30 to 122 eV we used 93 beams, from 126 to 162 eV we used 119 beams, and from 166 to 198 eV we used 147 beams. The Tb potential was calculated from relativistic charge densities kindly provided by N. E. Christensen; it should be pointed out that the CHANGE program calculates the phase shifts nonrelativistically, so that the theoretical curves presented here were obtained with nonrelativistic phase shifts calculated from a relativistic potential. We found, in fact, that for Tb the difference between $I(V)$ spectra calculated with relativistic and nonrelativistic phase shifts is small.

The inner potential was chosen initially to be $V_0 = -(10+4i)$ eV, but the real part was varied as a fitting parameter in the course of the analysis. The final value was $V_0 = -(7+4i)$ eV with an error of ± 3 eV in the real part. The amplitude of the atomic vibrations was taken as $\langle u^2 \rangle^{1/2} = 0.08$ Å, corresponding to a Debye temperature of 170 K.

The structure analysis concentrated on varying the first interlayer spacing d_{12} and the registration X of the top layer (see Sec. II). The changes in these parameters from the bulk values $d_{12} = 1.80$ Å and $X = a_1/6 = 1.04$ Å are labeled Δd_{12} and ΔX , respectively, a positive value of ΔX indicating shifts of atoms 1 and 1' along x away from the glide line, i.e., opposite to one another. The initial variations spanned large ranges: Δd_{12} from -0.40 to $+0.40$ Å in steps of 0.10 Å, and ΔX from -0.30 to $+0.30$ Å in steps of 0.10 Å. The refinement was done between -0.24 and $+0.08$ Å in steps of 0.02 Å for Δd_{12} and between 0 and $+0.35$ Å in steps of 0.05 Å for ΔX .

The evaluation of the fit between theory and experiment was done both visually and by means of three reliability factors, namely, R_{VHT} (Ref. 10), r_{ZJ} (Ref. 11), and R_P (Ref. 12). Contour plots of each of these three R factors in the Δd_{12} - ΔX plane are shown in Fig. 4, the minima being $R_P = 0.32$ for $\Delta d_{12} = -0.075$ Å and $\Delta X = +0.21$ Å; $r_{\text{ZJ}} = 0.17$ for $\Delta d_{12} = -0.050$ Å and

$\Delta X = +0.22$ Å; and $R_{\text{VHT}} = 0.18$ for $\Delta d_{12} = -0.055$ Å and $\Delta X = +0.21$ Å. These three results were averaged to produce the final values of the structural parameters as

$$\Delta d_{12} = -0.06 \pm 0.03 \text{ Å} \quad (3.3\% \text{ compression}),$$

$$\Delta X = +0.21 \pm 0.05 \text{ Å} \quad (20\% \text{ increase in } X),$$

with the same minimum values of the R factors as quoted above. The error bars have been estimated on the basis of earlier error analyses in LEED crystallography.¹³ Figures 5(a), 5(b), and 5(c) juxtapose the experimental and the theoretical $I(V)$ spectra calculated for the unrelaxed and the relaxed surface.

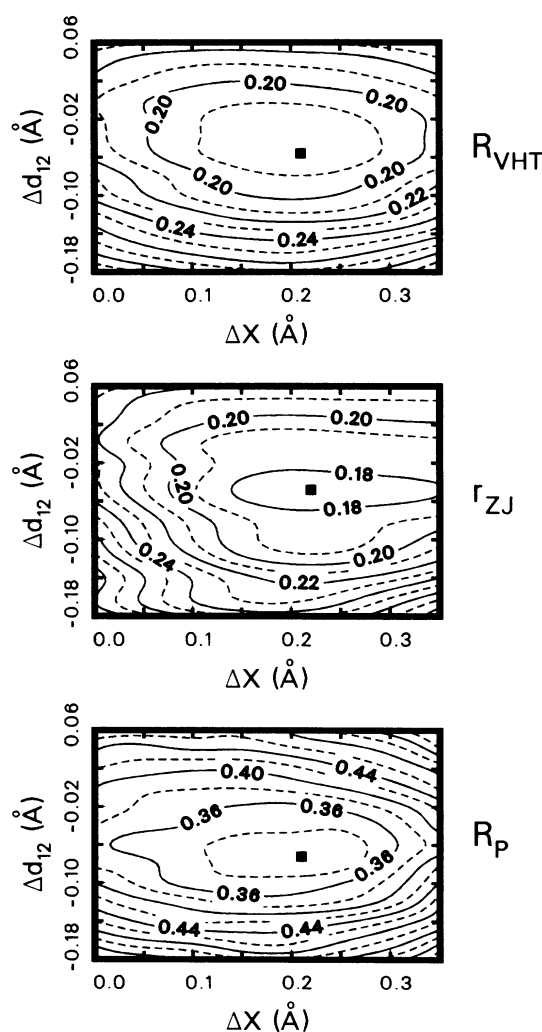


FIG. 4. Contour plots of the Van Hove-Tong R_{VHT} , the Zanazzi-Jona r_{ZJ} , and the Pendry R_P reliability factors. The minimum values, whose locations are indicated by the small squares, are given in the text.

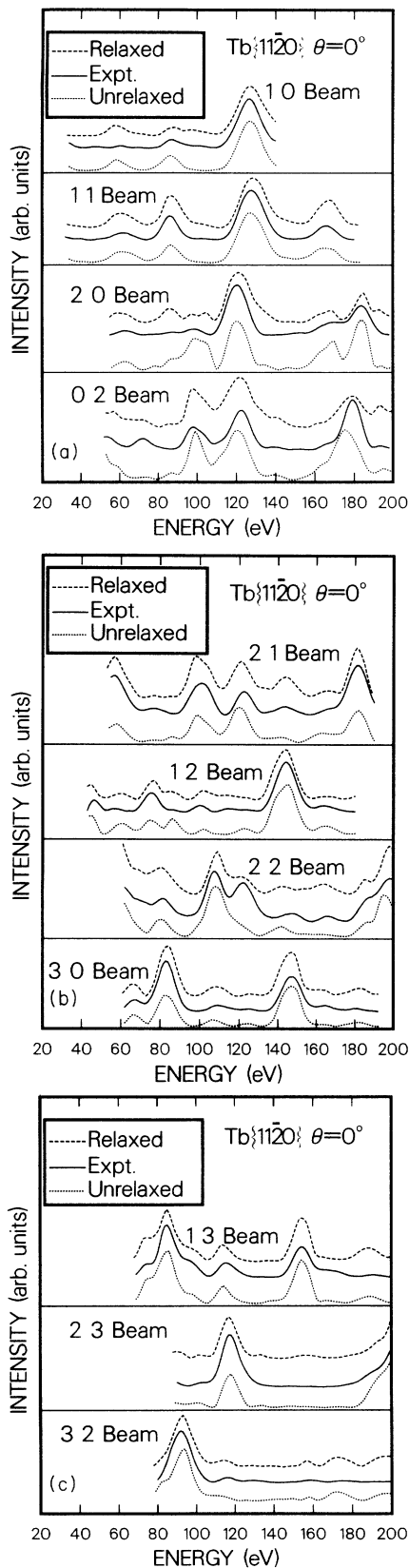


FIG. 5. Experimental (solid) and theoretical LEED $I(V)$ spectra for normal incidence on $\text{Tb}(11\bar{2}0)$. The theoretical curves were calculated for the relaxed (dashed) and the unrelaxed (dotted) surface structure.

V. DISCUSSION AND CONCLUSIONS

A quantitative LEED-intensity analysis finds that the $\text{Tb}(11\bar{2}0)$ surface is relaxed, with the first interlayer spacing contracted by 3.3% with respect to the bulk, and with the registration of the two sublayers in the top (composite) layer changed in such a way that the symmetry elements present on bulk $(11\bar{2}0)$ planes (a mirror and a glide line) are maintained.

In describing surface structure it is useful to maintain the distinction between relaxation, where the unit mesh of surface layers is preserved but each layer can translate with respect to bulk, and reconstruction, where the unit mesh of surface layers is changed and the symmetry is usually lowered. On $\text{Tb}(11\bar{2}0)$ we deal with the interesting case of relaxation of a composite layer made up of two elementary or Bravais nets which translate differently, and thereby change an internal structural parameter—the position vector of the second atom in the basis. This more general relaxation may be contrasted, on the one hand, with the relaxation of $\text{Co}(11\bar{2}0)$ (Ref. 7), which exhibits a contraction of 8.5% of the first interlayer spacing, but no parallel translation of either atom in the basis, i.e., no change of registration, and, on the other hand, with the still more general relaxation of $\text{GaAs}\{110\}$ (Ref. 14), where the Ga and As sublayers in the surface layers preserve the unit mesh, but translate differently in both the perpendicular and the parallel directions, thus producing a buckled surface. This rearrangement of surface atoms on $\text{GaAs}\{110\}$ is often called a reconstruction in the semiconductor literature, but that usage blurs the useful distinction between relaxation and reconstruction.

The present results differ from those reported for $\text{Y}(11\bar{2}0)$, $\text{Ho}(11\bar{2}0)$, and $\text{Er}(11\bar{2}0)$, which are reconstructed, by Blyth *et al.*⁴ and Barrett *et al.*⁴ One wonders whether indeed $\text{Tb}(11\bar{2}0)$ is intrinsically different from Y, Ho, and $\text{Er}(11\bar{2}0)$, or if the different surface-preparation procedures used could be responsible for the difference results. However, before speculating about the reasons for the differences, both types of result should first be confirmed by others with various experimental techniques, and more nonbasal planes of the rare earths should be investigated quantitatively.

ACKNOWLEDGMENTS

We acknowledge partial support of this work by the Department of Energy with Grant No. DE-FG02-86ER45239 and by the National Science Foundation with Grant No. DMR-8921123. The sample used in this work resulted from joint rare-earth-purification research at Birmingham and Iowa State Universities, funded by the U.K. Science and Engineering Research Council and by the U.S. Department of Energy, respectively. We are also indebted to D. Fort for providing the sample and to N. E. Christensen for providing the relativistic charge densities of Tb.

- ¹F. P. Netzer and J. A. D. Matthew, *Rep. Prog. Phys.* **49**, 621 (1986).
- ²B. J. Beaudry and K. A. Gschneidner, Jr., in *Handbook on the Physics and Chemistry of Rare Earths*, edited by K. A. Gschneidner, Jr. and L. Eyring (North-Holland, Amsterdam, 1987), Vol. 1, p. 173.
- ³D. Fort, *J. Less-Common Met.* **134**, 45 (1987).
- ⁴R. I. R. Blyth, R. Cosso, S. S. Dhesi, K. Newstead, A. M. Begley, R. G. Jordan, and S. D. Barrett, *Surf. Sci.* **251/252**, 722 (1991); S. D. Barrett, R. I. R. Blyth, A. M. Begley, S. S. Dhesi, and R. G. Jordan, *Phys. Rev. B* **43**, 4573 (1991), and references therein.
- ⁵S. Tougaard and A. Ignatiev, *Surf. Sci.* **115**, 270 (1982).
- ⁶J. Quinn, Y. S. Li, F. Jona, and D. Fort, *Surf. Sci.* **257**, L647 (1991).
- ⁷M. Welz, W. Moritz, and D. Wolf, *Surf. Sci.* **125**, 473 (1983).
- ⁸F. Jona, J. A. Strozier, Jr., and P. M. Marcus, in *The Structure of Surfaces*, edited by M. A. Van Hove and S. Y. Tong (Springer-Verlag, Berlin, 1985), p. 92.
- ⁹D. W. Jepsen, *Phys. Rev. B* **22**, 5701 (1980); **22**, 814 (1980).
- ¹⁰M. A. Van Hove, S. Y. Tong, and M. E. Elconin, *Surf. Sci.* **64**, 85 (1977).
- ¹¹E. Zanazzi and F. Jona, *Surf. Sci.* **62**, 61 (1977).
- ¹²J. B. Pendry, *J. Phys. C* **13**, 937 (1980).
- ¹³F. Jona, P. Jiang, and P. M. Marcus, *Surf. Sci.* **192**, 414 (1987).
- ¹⁴S. Y. Tong, A. R. Lubinski, B. J. Mrstik, and M. A. Van Hove, *Phys. Rev. B* **17**, 3303 (1978); B. J. Mrstik, S. Y. Tong, and M. A. Van Hove, *J. Vac. Sci. Technol.* **16**, 1258 (1979).

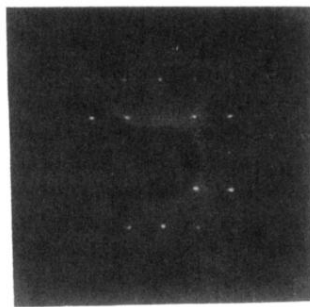


FIG. 3. Photograph of LEED pattern from clean Tb(11 $\bar{2}$ 0) for 56-eV incident electrons.